Applied Catalysis B: Environmental 125 (2012) 51–58

Contents lists available at SciVerse ScienceDirect

Applied Catalysis B: Environmental

journal homepage: www.elsevier.com/locate/apcatb

Fe-zeolites as heterogeneous catalysts in solar Fenton-like reactions at neutral pH

Rafael Gonzalez-Olmos[a,b,*], Maria J. Martin[a], Anett Georgi[b], Frank-Dieter Kopinke[b], Isabel Oller[c], Sixto Malato[c]

[a] Laboratory of Chemical and Environmental Engineering (LEQUiA), Institute of the Environment, University of Girona, Campus Montilivi s/n, Faculty of Sciences, E-17071 Girona, Spain
[b] Helmholtz Centre for Environmental Research – UFZ, Department of Environmental Engineering, Permoserstrasse 15, D-04318 Leipzig, Germany
[c] Plataforma Solar de Almería-CIEMAT, Ctra. Senés Km. 4, 04200-Tabernas, Almeria, Spain

ARTICLE INFO

Article history:
Received 25 March 2012
Received in revised form 18 May 2012
Accepted 18 May 2012
Available online 29 May 2012

Keywords:
Heterogeneous catalyst
Photo-Fenton
Zeolites
Phenol
Imidacloprid
AOP

ABSTRACT

This paper focuses on the study of photo-Fenton-like processes using two types of Fe-zeolites (Fe-ZSM5 and Fe-Beta) as heterogeneous catalysts in order to treat contaminated effluents with organic compounds at neutral pH. It was proved that light (solar and artificial) improves significantly the DOC removal in this kind of processes. A possible contribution by homogeneous photo-Fenton reaction catalyzed by the iron leached during the reaction was insignificant. This study also proves that the catalytic activity of Fe-zeolites is improved by photo Fenton-like processes using solar light in a pilot plant equipped with compound parabolic collectors (CPC).

1. Introduction

The increasing worldwide demand for clean water and the increasing presence of non-biodegradable pollutants in wastewaters have been the main reasons for the large number of studies focused on treatments by advanced oxidation processes (AOPs) [1–4] during the last years. AOPs are useful techniques for the treatment of toxic or non-biodegradable compounds such as pesticides, pharmaceuticals and other organic compounds in wastewater. In these types of processes the contaminants are converted into inorganic compounds such as water, CO_2, and salts, i.e. they undergo mineralization, or they are converted into oxygen-functionalized, short-chain molecules which are more easily biodegradable [5]. The main oxidant produced in AOPs is $OH^{\bullet}$.

The Fenton and photo-Fenton processes are known as effective AOPs to remove organic pollutants from wastewaters [6]. In these processes hydrogen peroxide together with dissolved iron produce reactive species, mainly $OH^{\bullet}$, which oxidize the organic compounds. The use of the homogeneous photo-Fenton reaction to oxidize organic contaminants in water has been extensively reported in the literature [2,7]. The mechanism in the photo-Fenton reaction is usually summarized by the following equations:

$$Fe^{2+} + H_2O_2 \rightarrow Fe^{3+} + OH^- + OH^{\bullet} \quad (1)$$

$$Fe^{3+} + H_2O_2 \rightarrow Fe^{2+} + HOO^{\bullet} + H^+ \quad (2)$$

$$Fe^{3+} + H_2O \xrightarrow{h\upsilon} Fe^{2+} + OH^{\bullet} + H^+ \quad (3)$$

$$H_2O_2 \xrightarrow{h\upsilon} 2OH^{\bullet} \quad (4)$$

$$OH^{\bullet} + H_2O_2 \rightarrow H_2O + HOO^{\bullet} \quad (5)$$

$$OH^{\bullet} + \text{Organic compounds} \rightarrow \text{Oxidized products} \quad (6)$$

In the presence of light, the rate of $OH^{\bullet}$ formation is increased by photoreactions of Fe^{3+} and photolysis of H_2O_2 which produce $OH^{\bullet}$ directly (Eqs. (3) and (4)) and regenerate Fe^{2+} [8].

On the contrary, Pignatello et al. [8] proposed that light enhances also the production of $OH^{\bullet}$ and ferryl species following additional mechanisms summarized in the following equations:

$$Fe^{3+} + H_2O_2 \rightarrow Fe - OOH^{2+} + H^+ \quad (7)$$

$$Fe - OOH^{2+} \xrightarrow{h\upsilon} Fe - OOH^{2+*} \quad (8)$$

$$Fe - OOH^{2+*} \rightarrow Fe^{2+} + HOO^{\bullet} \quad (9)$$

* Corresponding author at: Laboratory of Chemical and Environmental Engineering (LEQUiA), Institute of the Environment, University of Girona, Campus Montilivi s/n, Faculty of Sciences, E-17071 Girona, Spain.
E-mail address: rafael.gonzalez@udg.edu (R. Gonzalez-Olmos).

0926-3373/$ – see front matter © 2012 Elsevier B.V. All rights reserved.
http://dx.doi.org/10.1016/j.apcatb.2012.05.022

Table 1
Characteristic properties of the applied Fe-zeolites.[a]

Zeolite type	Framework code[b]	SiO_2/Al_2O_3 molar ratio	BET ($m^2\ g^{-1}$)	Maximum–Minimum pore diameter (Å)	Channel geometry	Particle size (μm)	Fe (wt%)
Fe-ZSM5	MFI	26	368	5.6–5.1	Parallel channels	0.95–12	2.1
Fe-Beta	BEA	42	602	7.7–5.6	3-D intersecting	0.4–2.0	1.0[c]

[a] The specific surface areas were determined by BET analysis using nitrogen, the SiO_2/Al_2O_3 ratios and Fe content were determined using X-ray fluorescence analysis and the particle size (lower limit d_{10}–upper limit d_{90}) was determined by laser diffraction analysis.
[b] Framework code of the International Zeolite Association (IZA)[20].
[c] Fe content after washing step.

$$Fe - OOH^{2+*} \rightarrow [Fe^{IV}{=}O]^{2+} + OH^{\bullet} \quad (10)$$

The main drawbacks in photo-Fenton and Fenton processes are that the use of dissolved iron as catalyst requires its subsequent removal from the treated water, mostly as iron oxyhydroxide sludge, and the necessity of working at low pH (around pH 3) to keep iron in solution and achieve acceptable conversion rates. For this reason, in the last years an important effort has been done in the field of heterogeneous catalysis in order to be able of working in wider pH ranges and also to facilitate the reuse of iron [5,9]. Among the different catalysts used in heterogeneous Fenton-like reactions, Fe-containing zeolites have shown high catalytic activities in the oxidation of organic compounds, with minimal iron leaching [5,10,11]. Several studies have used artificial UV light to convert the heterogeneous Fenton-like process with Fe-zeolites, in a heterogeneous photo-Fenton-like process [12–18]. A few of these studies have explored the use of solar light as irradiation source. In fact, there is just one paper reported by Rios-Enriquez et al. [19] in which the authors worked with solar light using Fe-Y zeolite to oxidize 2,4-xylidine at pH 3.

Therefore, the objectives of this study are to give more evidences about the activity of Fe-zeolites in heterogeneous photo-Fenton-like reactions at near neutral pH and to study solar light as irradiation source in these processes. This study quantifies the contribution of homogeneous Fenton and photo-Fenton reactions catalyzed by the iron leached during the process. Finally, Fe-zeolites were tested in a heterogeneous photo-Fenton-like process using compound parabolic collectors (CPC) with solar light in a pilot plant obtaining promising results.

2. Materials and methods

2.1. Chemicals and reagents

All chemicals used and organic solvents (purity higher than 99%) as well as H_2O_2 solution (30%) were obtained from Merck (Germany). All solvents used for chromatography, acetonitrile, methanol, and ultrapure (MilliQ) water, were high-performance liquid chromatography (HPLC) grade. The filters used were syringe-driven 0.2 mm Millex nylon membrane filters from Millipore. Demineralised water used was supplied by the Plataforma Solar de Almería (PSA) distillation plant (conductivity <10 μS cm^{-1}, $[Cl^-] = 0.7–0.8\ mg\ L^{-1}$, $[NO_3^-] = 0.5\ mg\ L^{-1}$, organic carbon <0.5 mg L^{-1}). The applied Fe-zeolites were provided by Süd-Chemie Zeolites (Bitterfeld, Germany). In order to minimize the Fe leaching from Fe-Beta, it was washed prior to application in reactions following the procedure described in our previous study [10]. The characteristics of zeolites (type, framework code, SiO_2/Al_2O_3 ratio, BET surface area, maximum and minimum pore diameter, particle size, and the percentage of immobilized iron) were summarized in Table 1.

2.2. Analytical procedures

Dissolved organic carbon (DOC) was measured by direct injection of samples filtered with 0.2 μm syringe-driven filters into a Shimadzu–5050A TOC analyzer. The relative standard deviation of the DOC method is in the range of <3.6%.

Colorimetric determination of total iron concentration was performed with 1,10-phenantroline according to ISO 6332. Hydrogen peroxide was analyzed by a spectrophotometric method using titanium (IV) oxysulfate (DIN 38 402 H15 method), which forms a yellow complex with H_2O_2 (maximum absorption at 410 nm).

HPLC (Agilent Technologies, series 1100) was used to monitor the phenol and imidacloprid concentrations with a UV-DAD detector and a C-18 column (LUNA 5 μm, 3 mm × 150 mm from Phenomenex) at 30 °C. The relative standard deviation of the phenol determination was <3.5% and for imidacloprid <4.4%.

Concentrations of dichloroacetic acid (DCAA) and other carboxylic acids were determined with a Dionex DX 600 ion chromatography (IC) system using a Dionex Ionpac AS11-HC column (4 mm × 250 mm). The ammonium and amines (methylamine, ethylamine, diethylamine, propylamine) concentrations were measured with an 850 Professional IC system (Metrohm) equipped with conductivity detector and a Metrosep C4 column (4 mm × 250 mm). The relative standard deviation of the IC determinations was in the range of <5.0%.

The data presented, i.e. residual concentrations of the individual compounds and DOC, represent mean values of at least two replicate experiments. The deviation of the individual values from the mean value was generally lower than 10%.

2.3. Solar simulator procedure

The photodegradation experiments with simulated solar radiation were performed in beakers of 2 L in a solar light simulator (suntest, XLS+ Heraeus, Germany), equipped with a 2.2 kW xenon arc lamp and special filters restricting transmission of light below 290 nm. The lamp power can be adjusted between 250 and 765 W m^{-2} in the range of 290–800 nm (9% correspond to UV radiation in the range from 290 to 400 nm). The intensity of radiation was maintained constant during all experiments at 765 W m^{-2} between 290 and 800 nm (68.85 W m^{-2} in the UV range). Temperature was monitored during all experiments and it varied around 35 ± 2 °C. Both, batch-experiments for Fenton (dark conditions) and photo-Fenton (light conditions) processes, were prepared by adding a determined amount of Fe-zeolite (Fe-ZSM5 or Fe-Beta) to 1000 mL of a solution of 50 mg L^{-1} of one of the target compounds (phenol, imidacloprid or DCAA). The aqueous suspension containing the target compound and Fe-zeolite was stirred and allowed to reach the adsorption equilibrium within 24 h. Afterwards, the concentration of the target compound in the solution phase was measured by the explained analytical methods. Because of the surface acidity of the two catalysts, the initial pH (pH_0) of the zeolite suspension was around 5 and it was adjusted to 7 by adding dilute NaOH and monitored during the experiment. Fenton-like reaction was then

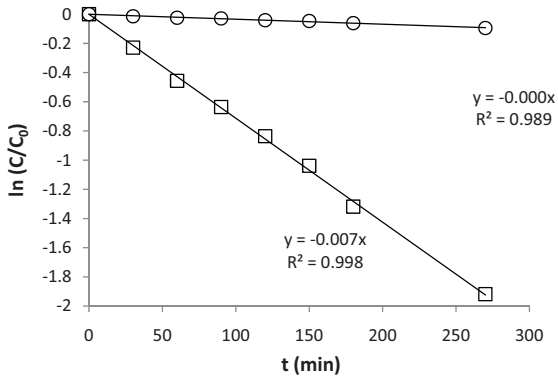

Fig. 1. Decomposition of H_2O_2 (C_0 = 1 g L^{-1}) in catalyst suspensions ($C_{zeolite}$ = 2 g L^{-1}) of Fe-ZSM5 (□) and Fe-Beta (◯) with artificial solar light.

started by adding 0.3 or 1.0 g L^{-1} of H_2O_2 and this concentration was kept constant during the process by adding H_2O_2 periodically. In order to determine residual concentrations of the target compounds during the experiments, 25 mL aliquots of the suspension were sampled and spiked with 0.44 mmol of sodium thiosulfate in order to stop the reaction (complete consumption of H_2O_2). For HPLC analyses, 5 mL aliquots were mixed with 5 mL of methanol (in experiments with phenol) or acetonitrile (in experiments with imidacloprid) and shaken for 2 h in order to extract the adsorbed compound fraction into the solution phase for injection into HPLC system. The extraction recovery was higher than 95% and 97% for phenol and imidacloprid, respectively. In order to assess the influence of light, Fenton-like dark reactions with the Fe-zeolites were done in the same way adjusting the temperature also to 35 ± 2 °C.

2.4. Solar pilot plant procedure

Heterogeneous photo-Fenton experiments at neutral pH were performed at the Plataforma Solar de Almería, Spain (PSA, latitude 37°N, longitude 2.4°W) in a solar pilot plant based on CPC specially designed for solar photocatalytic applications. In order to perform reactions under dark conditions the CPC were covered with sheet metal plates. The reactor is composed of two 11 L modules with twelve Pyrex glass tubes (30 mm O.D.) mounted on a fixed platform tilted 37° (local latitude). The water flowed (20 L min^{-1}) directly from one module to the other and finally to a 7 L reservoir. The piping and valves (3 L) between the reactor and the tank were from black HDPE, which is highly resistant to chemicals, weatherproof and opaque, preventing any photochemical effect from outside the collectors. The total illuminated area was 3 m^2, the total volume (two modules + reservoir tank + piping and valves) was 32 L (V_t) and the irradiated volume was 22 L (V_i). Solar ultraviolet radiation (UV) was measured by a global UV radiometer (KIPP&ZONEN, model CUV 3) mounted on a platform tilted 37° the same as the CPC. The temperature inside the reactor was continuously recorded by a temperature probe (Crioterm PT-100 3H) inserted in the piping. A plant diagram has been published elsewhere [21]. Combination of data from several experimental days and their comparison with other photo-Fenton-like experiments is possible by means of Eq. (11),

$$t_{30W,n} = t_{30W,n-1} + (t_n - t_{n-1})\frac{UV}{30\ [W\ m^{-2}]}\frac{V_i}{V_t} \quad (11)$$

where t_n is the effective treatment time for each sample, UV is the average solar ultraviolet radiation power density [W m^{-2} at λ < 400 nm] measured between t_{n-1} and t_n, and $t_{30W,n}$ is a "normalized illumination time" [22]. In this case, illumination time refers to a constant solar UV power of 30 W m^{-2} (typical solar UV power density on a perfectly sunny day around noon). The time course of temperature was nearly identical for the experiments presented in this study. The temperature increased from (13 ± 2) °C before start of illumination to (36 ± 3) °C. In the dark experiments the increase of temperature was from (13 ± 2) °C to (27 ± 3) °C. The scattering in residual concentrations of the individual compounds and the DOC concentration, determined as deviation of the individual values of replicate experiments from their mean value, was generally in the range of 2–15%.

3. Results and discussion

3.1. Decomposition of H_2O_2 with light and Fe-zeolites

Fig. 1 shows that the decomposition of H_2O_2, using Fe-ZSM5 and Fe-Beta in the solar simulator, follows a pseudo first-order kinetics. The catalytic activity (A) is calculated with Eq. (12)

$$A = \frac{k_1}{C_{cat}} \quad (12)$$

where k_1 [min^{-1}] is the pseudo first-order rate constant and C_{cat} [g L^{-1}] the catalyst concentration. In the experiment with Fe-ZSM5 an activity of $A = 3.6 \times 10^{-3}$ L g^{-1} min^{-1} was obtained. This value is identical with that obtained in our previous study [10] under dark conditions (3.7×10^{-3} L g^{-1} min^{-1}). The catalytic activity of Fe-Beta for H_2O_2 decomposition under the same conditions was 1.5×10^{-4} L g^{-1} min^{-1}, one order of magnitude lower than for Fe-ZSM5. On the contrary, the catalytic activity of Fe-Beta for H_2O_2 decomposition increased by a factor of 5 compared to the value under dark conditions (3.0×10^{-5} L g^{-1} min^{-1}) [10]. The prevailing assumption in the literature is that H_2O_2 is decomposed at the iron sites in the zeolite by a Fenton type mechanism whereby hydroxyl radicals are formed [23]. But other mechanisms related with the formation of high valent oxoiron complexes such as ferryl may be involved as well [24]. It should be kept in mind, that H_2O_2 is consumed via 'productive' pathways leading to highly reactive species like OH• or ferryl and 'non-productive' pathways, according to, e.g. Eqs. (2) and (5). Thus a high catalytic activity for H_2O_2 decomposition is not necessarily equivalent to fast contaminant degradation as will be shown below. In addition, even though there was no significant enhancement in H_2O_2 decomposition induced by light in case of Fe-ZSM5, a positive effect on the rate of reactive species formation cannot be excluded since it could be hidden by a high contribution of the non-productive pathway to the observed H_2O_2 decomposition.

As we mentioned in our previous study [24] the catalytic activity for H_2O_2 under dark conditions cannot be simply explained by the difference in the total Fe content in the catalyst (which is only about a factor of two) between the Fe-zeolites used in this study (Table 1). In fact, the speciation of the iron in the zeolite cages has to be considered as an important factor as well. This might be also the reason why the iron in the Beta zeolite is more sensitive to activation by light. The lower particle size of the Beta compared to the ZSM5 zeolite might also play a role improving the light penetration into the particles. However, in order to elucidate the differences in type and steric properties of the iron coordination in the Fe-zeolites sophisticated experimental and modeling approaches would be required which are not in the scope of this work.

3.2. Effect of light in heterogeneous photo-Fenton reaction using Fe-zeolites

In order to assess the effect of light in Fenton-like reactions catalyzed by Fe-zeolites, experiments on phenol degradation in the dark and under artificial solar light at pH_0 7 were carried out with Fe-ZSM5. In both types of reactions, phenol degradation

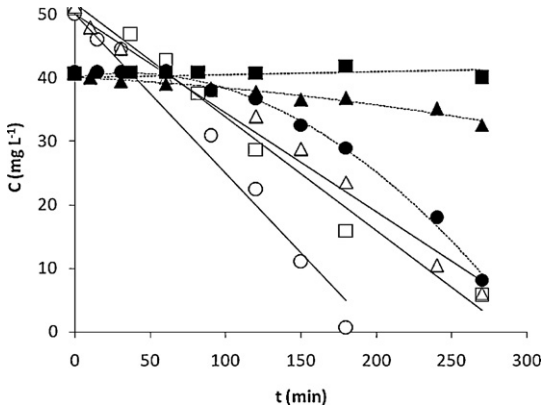

Fig. 2. Catalytic phenol degradation in the dark (△) and with artificial solar light (○) and DOC removal in the dark (▲) and with artificial solar light (●) using H_2O_2/Fe-ZSM5 ($C_{zeolite}$ = 2 g L^{-1}). Phenol degradation (□) and DOC removal (■) with artificial solar light catalyzed by leachate (C_{Fe} = 0.3 mg L^{-1}) from Fe-ZSM5. $C_{phenol,0}$ = 50 mg L^{-1}; pH$_0$ 7; $C_{H_2O_2}$ = 0.3 g L^{-1}. Here and in all other figures, filled symbols always represent DOC results and open symbols the individual compound concentrations. The lines for DOC were drawn as guides to the eye. Lines for phenol represent fitting to zero-order kinetics.

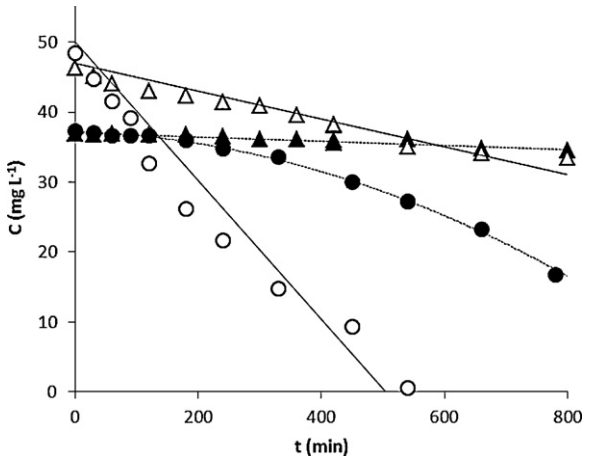

Fig. 3. Catalytic phenol degradation in the dark (△) and with artificial solar light (○) and DOC removal in the dark (▲) and with artificial solar light (●) using H_2O_2/Fe-Beta. $C_{phenol,0}$ = 50 mg L^{-1}; $C_{zeolite}$ = 2 g L^{-1}; pH$_0$ 7; $C_{H_2O_2}$ = 1 g L^{-1}. The lines for DOC were drawn as guides to the eye. Lines for phenol represent fitting to zero-order kinetics.

approximately follows a zero-order kinetics. This finding can be interpreted in terms of the ratio between the rates at which reactive species are formed and consumed, respectively. Zero-order kinetics indicates that the consumption of reactive species is much faster than their production, so that the rate of degradation of the organic compounds finally only depends on the rate of reactive species formation which can be constant during the reaction since the concentration of H_2O_2 was kept at a constant level.

According to Fig. 2, in the presence of light, phenol disappeared about 1.6 times faster than in the dark (zero-order rate constants: 0.25 mg L^{-1} min^{-1} and 0.15 mg L^{-1} min^{-1} for the reaction under solar light and dark conditions, respectively). On the contrary, the degree of DOC mineralization was much higher when light was used. After 270 min under dark conditions DOC was reduced by 20% only while using light by more than 80%. In both reactions the iron leaching was lower than 1% (0.3 mg L^{-1}). Nevertheless, the possible contribution of a photo-Fenton reaction catalyzed by dissolved iron needs to be checked. Therefore, a separate experiment was carried out with the filtrated water phase of an aqueous suspension of Fe-ZSM5 (2 g L^{-1}) that was stirred for 24 h. About 0.3 mg L^{-1} of dissolved iron was detected in this filtrate. Fig. 2 shows that the DOC content remained constant during the reaction in the leaching solution, while the phenol concentration decreased. It is not likely that Fenton-like processes are efficient at circumneutral conditions. Taking into account the results of Bali et al. [25] on the photolysis of phenol (100 mg L^{-1}) in the presence of H_2O_2 (0.3 g L^{-1}), a reaction mechanism without participation of iron species appears more likely. In any case, more significant results were obtained with respect to the DOC removal. The leachate was not able to effect a significant mineralization, comparable to Fe-ZSM5. This may be due to different production rates of reactive oxidant species or different species patterns. The results of these experiments reinforce the hypothesis that the iron inside the zeolite is mainly responsible for the catalytic activity in the process and that light produces a positive effect enhancing the compound degradation and DOC abatement. It is well known, from interference microscopy (IFM) studies [26], that zeolite crystallites are transparent for light in the wavelength range of 300–550 nm. Thus light could reach the Fe sites in this wavelength range.

Fig. 3 shows the degradation of phenol using Fe-Beta under dark conditions and with artificial solar light. In order to decrease the reaction time, the H_2O_2 concentration was increased up to 1 g L^{-1} (compared to 0.3 g L^{-1} in the experiments described above). The reaction rates for phenol degradation were 0.10 mg L^{-1} min^{-1} and 0.02 mg L^{-1} min^{-1} in experiments using light and dark conditions, respectively. The DOC content at the end of these experiments (800 min) was reduced by 60% in the illuminated experiments and only 7% in the dark. Obviously, Fe-Beta is more sensitive to light effects for phenol degradation, as was also observed in the H_2O_2 decomposition experiments.

3.3. Adsorption of organic target compounds into Fe-zeolites

Compounds with different hydrophobicity, molecular size and reactivity toward OH• were used in this study (Table 2). The percentage of adsorption for phenol (small aromatic compound, medium hydrophobicity), imidacloprid (large aromatic molecule, low hydrophobicity), DCAA (aliphatic, high polarity) into the two Fe-zeolites at the initial reaction conditions was determined ($C_{zeolite}$ = 2 g L^{-1}; $C_{compound,0}$ = 50 mg L^{-1}). Phenol presents a similar adsorption degree with both zeolites (around 10–15%). Imidacloprid, the largest molecule in this study, was strongly adsorbed by Fe-Beta (98%), the zeolite with the larger pore diameter, but almost not adsorbed by Fe-ZSM5. It is remarkable, that the adsorption degree of imidacloprid with Fe-Beta is much higher than for phenol, despite its lower hydrophobicity. DCAA, which is present as an anion under the experimental conditions (pK_a = 1.25) was not significantly adsorbed by any of the two zeolites. These results illustrate that adsorption into zeolites is controlled not only by hydrophobicity of substrates but also by specific interactions, in particular by the fitting between target molecules and zeolite channels and cages. The results discussed in the following sections will permit to evaluate the efficiency of each catalyst for various contaminants, enhancing our knowledge about the application range of this heterogeneous photo-Fenton-like process.

3.4. Heterogeneous photo-Fenton degradation of the target compounds using Fe-zeolites

Fig. 4a shows the degradation of various compounds used in this study with Fe-ZSM5, H_2O_2 and artificial solar light at initially neutral pH. Phenol showed the best results in terms of compound degradation (complete degradation after 100 min of reaction) and DOC removal (about 90% after 180 min of reaction). This is in accordance with the fact that this compound has the highest reactivity with respect to OH• (k_{OH} = 1.8 × 10^{10} L mol^{-1} s^{-1}) and showed

Table 2
Characteristic properties of the applied target compounds: Chemical structure, octanol-water partition coefficient (K_{ow}) and rate constant for the reaction with hydroxyl radicals (k_{OH}).

Compound	Formula	$\log K_{ow}$[a]	k_{OH} (10^8 L mol^{-1} s^{-1})[b]
Phenol	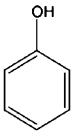	1.46	180
Imidacloprid	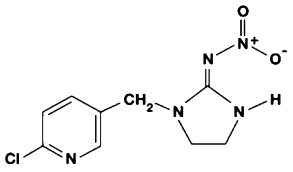	0.57	43[c]
Dichloroacetic acid (DCAA)	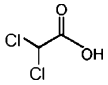	0.92	0.92[d]

[a] [27].
[b] [28].
[c] [29].
[d] Value for dichloroacetate because DCAA was dissociated at reaction pH.

the highest adsorption degree with this zeolite. Imidacloprid ($k_{OH} = 4.3 \times 10^9$ L mol^{-1} s^{-1}) was removed more slowly than phenol (≈98% degradation in 420 min) and its DOC was reduced after 800 min by only 43%. Finally, DCAA was removed with a much lower rate than the two other compounds. DCAA has the lowest adsorption degree and reactivity toward OH• ($k_{OH} = 9.2 \times 10^7$ L mol^{-1} s^{-1} for dichloroacetate). DCAA was degraded by 65% in 800 min, at the same time the DOC was reduced by 63%. This indicates that the compound was directly mineralized without formation of long-living intermediates. This is in agreement with results obtained by Salazar et al. [30]. Furthermore, the chloride ion formation also gives evidence that the reaction does not produce stable intermediates since it corresponds closely to the time course of DCAA conversion. At the end of the reaction, chloride recovery was (94 ± 3)%. The different apparent reaction orders with respect to contaminant concentration observed for phenol (zero order), imidacloprid and DCAA (both approximately first order) can possibly be explained by the differences in the rate of consumption of reactive species. The higher the reactivity of the compound, the higher is the rate of consumption of reactive species. In case of a fast consumption of reactive species, their formation becomes the rate limiting step, i.e. zero order kinetics with respect to the compound concentration. In case of slow consumption, the concentration of reactive species can reach a steady state, which under certain preconditions can lead to an apparent first-order kinetics for contaminant degradation. Based on the products of compound concentration times rate constant for reaction with OH• ($k_{OH} \times C_{consumer}$) it is possible to reveal the dominant consumer of OH• in a reaction system. Such a simple approach disregards local enrichment of any compound near the catalytic center. In case of DCAA, the compound reactivity is so low that H_2O_2 most likely is the dominant consumer of OH• in the system. Thus, the steady-state concentration of OH• is independent of the contaminant concentration, resulting in pseudo-first order kinetics.

At the end of the photoreaction with phenol, the degradation products in the aqueous solution were analyzed and compared to those obtained in a similar reaction under dark conditions. The results showed that the mineralization of phenol under irradiation was more complete. Oxalic acid was not present in the experiments with light. This finding supports the hypothesis that Fe-oxalate complexes, which are almost inert under dark conditions, can be more easily degraded under irradiation via a photo-induced ligand-to-metal electron transfer [31]. The concentration of other carboxylic acids was also rather high in the experiments in the dark and very low under irradiation. This is clearly one step forward to overcome the limitations of conventional Fenton-like systems: carboxylic intermediates can hardly be degraded thus preventing high degrees of DOC removal. Various carboxylic acids (especially dicarboxylic acids) are known to form stable iron complexes, which inhibit the reaction with peroxide [32]. Photo-Fenton is able to drive the catalytic iron cycle even when redox-active organic intermediates (e.g. quinones [8]) are depleted already and relatively stable ligands (such as carboxylic acids) dominate. This makes the photo-Fenton system in particular efficient in the final stage of a sequence of oxidation reactions.

Fig. 4b shows the results of phenol and imidacloprid heterogeneous photo-Fenton oxidation with artificial solar light using Fe-Beta. For this study DCAA was discarded due to the long reaction time needed to reach complete degradation. With Fe-Beta the degradation of phenol was slower than with Fe-ZSM5. The reaction rates for phenol degradation were 0.10 and 0.52 mg L^{-1} min^{-1} in experiments using Fe-Beta and Fe-ZSM5, respectively. After 800 min the DOC concentration was reduced by 60% in the experiments with Fe-Beta. The degradation of imidacloprid in the presence of Fe-Beta followed a pseudo first-order kinetics. The degradation rate for imidacloprid was slightly higher with Fe-Beta than with Fe-ZSM5, despite the fact that Fe-Beta presents a lower reactivity for H_2O_2 decomposition and for phenol degradation. The pseudo-first order rate constants for imidacloprid degradation were 0.067 min^{-1} and 0.094 min^{-1} for Fe-ZSM5 and Fe-Beta, respectively. The main reason for the fast reaction of imidacloprid with Fe-Beta might be its high degree of adsorption (≈99%). So the lower intrinsic catalytic activity of Fe-Beta compared to Fe-ZSM5 is compensated by the higher enrichment of imidacloprid in the vicinity of the catalytic sites of Fe-Beta leading to higher local concentrations. In the case of Fe-Beta, the DOC concentration, which is measured in the solution phase, was initially close to zero due to adsorption and went through a maximum during the course of the reaction. This is explained by desorption of some degradation products. Among the degradation products, organic acids (formic, pyruvic, acetic, oxalic acid) and amines (methylamine, ethylamine) were detected with ion chromatography.

Table 3 shows the H_2O_2 consumption required to reduce the initial concentration of contaminants by 50% (H_2O_{2cons}) in the

Table 3
Compound degradation in heterogeneous photo-Fenton-like reaction using artificial light with solar simulator. H_2O_2 consumption for 50% contaminant degradation (H_2O_{2cons}), half-life of compound ($t_{0.5}$), initial pH–final pH (pH_0–pH_f), half-life of DOC ($t_{DOC0.5}$) at $C_{compound,0}$ = 50 mg L^{-1}; $C_{H_2O_2}$ = 1 g L^{-1}; $C_{zeolite}$ = 2 g L^{-1}.

	Fe-ZSM5				Fe-Beta			
	H_2O_{2cons} (mg L^{-1})	$t_{0.5}$ (min)	pH_0–pH_f	$t_{DOC0.5}$ (min)	H_2O_{2cons} (mg L^{-1})	$t_{0.5}$ (min)	pH_0–pH_f	$t_{DOC0.5}$ (min)
Phenol	432	38	7.0–4.9	105	70	200	7.0–5.7	830
Imidacloprid	895	132	7.1–4.1	>1500	45	105	7.0–4.8	1200

heterogeneous photo-Fenton process. It is remarkable that Fe-ZSM5 consumed around 6 times more H_2O_2 than Fe-Beta in case of phenol oxidation. This indicates that despite the faster reaction with Fe-ZSM5, the efficiency in the utilization of H_2O_2 is less. For imidacloprid the 50% H_2O_2 consumption was even 20 times higher with Fe-ZSM5 than with Fe-Beta. In this case the higher adsorption of imidacloprid in Fe-Beta significantly contributes to the improvement in the H_2O_2 utilization efficiency. The positive effect of adsorption on contaminant degradation has been described also for reactions under dark conditions using the two Fe-zeolites [10,11].

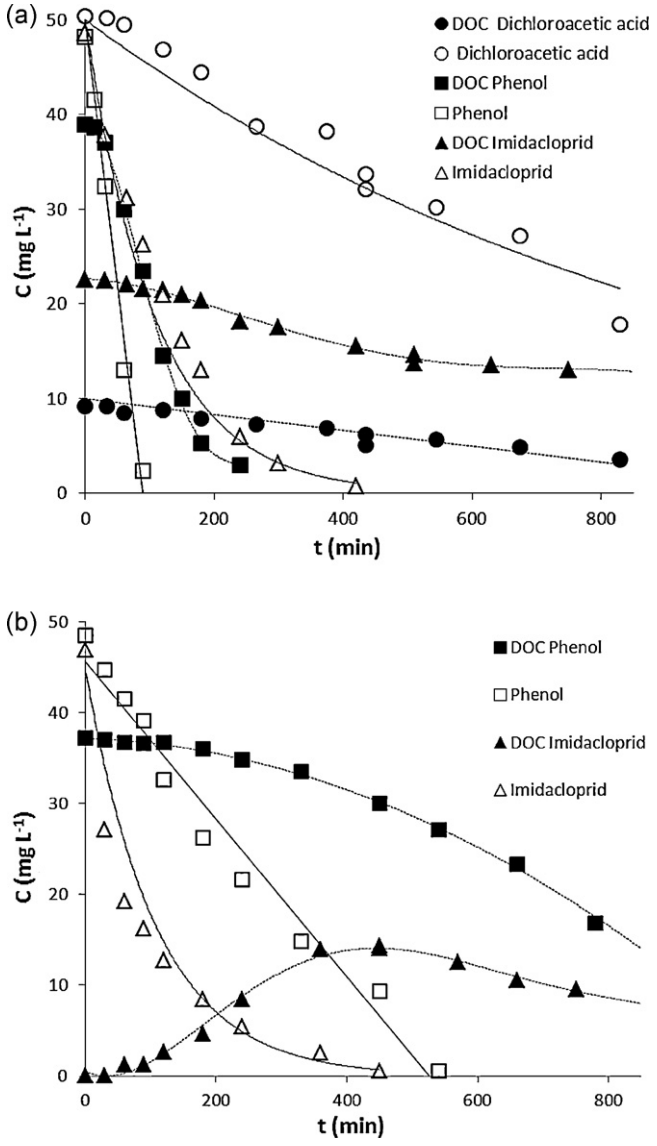

Fig. 4. Heterogeneous photo-Fenton oxidation of target compounds with Fe-ZSM5 (a) and Fe-Beta (b) using artificial light in solar simulator. $C_{compound,0}$ = 50 mg L^{-1}; $C_{Fe\text{-}ZSM5}$ = 2 g L^{-1}; pH_0 7; $C_{H_2O_2}$ = 1 g L^{-1}. The lines for DOC were drawn as guides to the eye. Lines for phenol represent fitting to zero-order kinetics and for imidacloprid and DCAA represent fitting to first-order kinetics.

During the oxidation reactions a decrease of pH toward values between 4.1 and 5.7 was observed. This is due to the formation of by-products such as organics acids. If the pH is kept constant during the reaction by periodic addition of NaOH, the rate of phenol degradation is slightly lower, i.e. >95% of phenol degradation are reached only after 110 min of reaction compared to 80 min in experiments with decline in pH (experiments with $C_{zeolite}$ = 2 g L^{-1}, $C_{H_2O_2}$ = 1 g L^{-1}). The DOC half-life was increased from 100 min to 200 min (a factor of 2) when pH was kept constant during reaction. This finding is important with respect to application of photo-Fenton systems on real wastewaters which are usually buffered.

3.5. Solar heterogeneous photo-Fenton test in a pilot reactor using solar light

In order to test the Fe-zeolites in a CPC reactor where solar light was used as irradiation source, the most reactive compound phenol was selected as a target compound. The experiments were done at pH_0 7 during December–January when the sun radiation is low. Fig. 5a shows the evolution of phenol concentration over normalized irradiation time. Prior to the start of reaction an initial operation period of 30 min was conducted in order to facilitate phenol adsorption into the zeolite. Then H_2O_2 was added and illumination was started. Different iron concentrations in form of Fe-ZSM5 between 20 and 100 mg L^{-1} were used, corresponding to Fe-ZSM5 concentrations of 1–5 g L^{-1}. For all applied catalyst concentrations a significant positive effect of irradiation was observed.

Fig. 5b shows the zero-order rate constants (mg L^{-1} min^{-1}) and the time needed to reduce 50% of the initial DOC concentration ($t_{DOC,0.5}$) in the experiments with solar light and under dark conditions. For the irradiation experiments, the real time scale is transformed into the normalized irradiation time ($t_{30W,n}$) according to Eq. (11). There is a strong increase in the rate constants for phenol degradation with increasing catalyst concentration. The effect for DOC half-life is lower. The correlation between rate constants and catalyst concentrations is almost linear for the dark reaction, but clearly nonlinear for the irradiation experiments. This is due to the increased optical density of the suspension at higher zeolite concentrations, i.e. a shading effect. A direct comparison of the degradation rate constants for the CPC experiments under solar light and dark conditions is not that straightforward as in case of the laboratory experiments. This is due to the slight differences in reaction temperatures (see Section 2), but also due to the normalized time scale in order to account for natural variations in irradiation intensity. This approach leads to an underestimation of the contribution of the dark reaction compared to the light-driven reaction. Nevertheless, the data presented in Fig. 5b show the same trends as the laboratory experiments using artificial solar light: a moderate acceleration of phenol degradation by irradiation (a factor of 2 in the rate constants) and a more pronounced effect on DOC removal rates (a factor of 4 in $t_{DOC,0.5}$).

Fig. 6 shows similar experiments with Fe-Beta in the CPC photo-reactor. In this case experiments with two different iron concentrations (20 and 40 mg L^{-1}, corresponding to Fe-Beta concentrations of 2 and 4 g L^{-1}) were carried out. The phenol

Table 4
Phenol degradation using solar light in the CPC reactors: H_2O_2 consumption for 50% contaminant degradation (H_2O_{2cons}), half-life of phenol ($t_{0.5}$), initial and final pH (pH_0–pH_f), half-life of DOC ($t_{DOC0.5}$) at $C_{phenol,0}$ = 50 mg L^{-1}; $C_{H_2O_2}$ = 1 g L^{-1}.

	Fe-ZSM5				Fe-Beta			
Fe (mg L^{-1}) in zeolite	H_2O_{2cons} (mg L^{-1})	$t_{0.5}$ (min)	pH_0–pH_f	$t_{DOC0.5}$ (min)	H_2O_{2cons} (mg L^{-1})	$t_{0.5}$ (min)	pH_0–pH_f	$t_{DOC0.5}$ (min)
20	183	57	7.0–3.4	100	93	90	7.0–5.2	n.d.
40	354	17	7.0–5.0	49	155	60	7.0–4.4	n.d.
100	703	7	7.0–5.3	40				

n.d. = not determined.

degradation rate was increased by a factor of 1.3 when the iron concentration was increased by a factor of 2. The fraction of phenol adsorbed at t = 0 (28% and 48% for 2 and 4 g L^{-1} Fe-Beta, respectively, as illustrated by the decrease in DOC at t = 0, shown in Fig. 6) was higher by a factor of about 2 compared to the laboratory experiments. This is mainly due to the adsorption temperature which was 35 °C in the lab experiments compared to 10 °C in the pilot experiments. Again, phenol degradation and mineralization were slower with Fe-Beta than with Fe-ZSM5. The course of the DOC concentration in the CPC experiment with Fe-Beta reflects the superposition of desorption of more hydrophilic intermediates from the zeolite and actual reduction of DOC due to mineralization. Much longer reaction times would be required in order to further decrease the DOC. On the contrary and according to the results shown in Table 4, H_2O_2 was consumed more efficiently in CPC photo-reactor

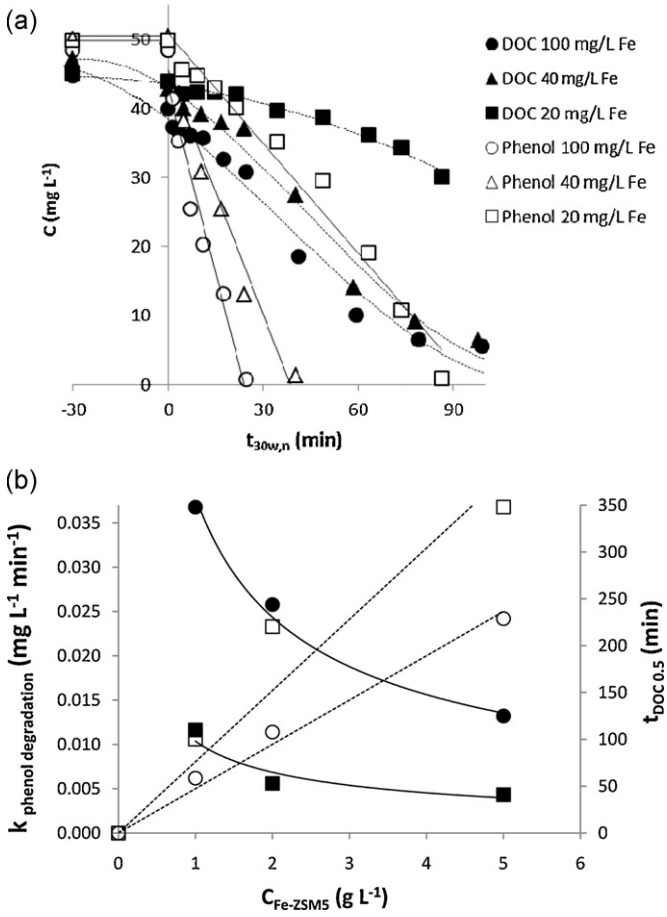

Fig. 5. (a) Phenol degradation and DOC removal using Fe-ZSM5 and solar light in CPC pilot plant. C_{Fe} = 20–100 mg L^{-1}; $C_{phenol,0}$ = 50 mg L^{-1}; pH_0 7; $C_{H_2O_2}$ = 1 g L^{-1}. (b) Zero-order kinetics rate constant in the dark (○) and with solar light (□) and time needed to reduce the initial DOC concentration by 50% in experiments in the dark (●) and with solar light (■). The lines for DOC were drawn as guides to the eye. Lines for phenol represent fitting to zero-order kinetics.

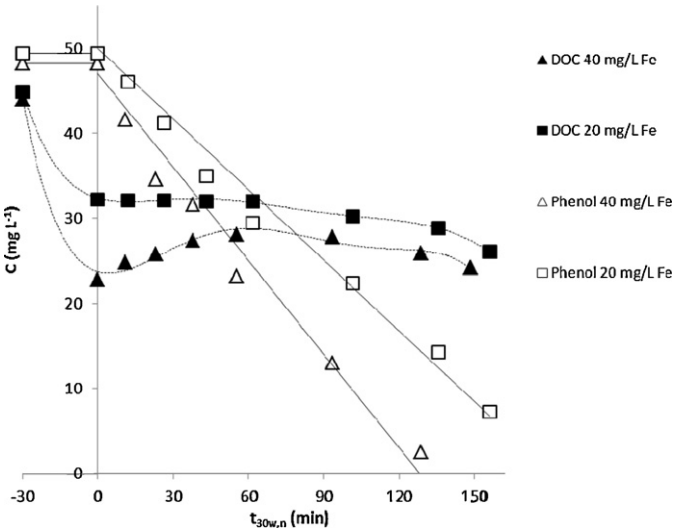

Fig. 6. Phenol degradation and DOC removal using Fe-Beta and solar light in CPC pilot plant. Fe-Beta: C_{Fe} = 20–40 mg L^{-1}; $C_{phenol,0}$ = 50 mg L^{-1}; pH_0 7; $C_{H_2O_2}$ = 1 g L^{-1}. The lines for DOC were drawn as guides to the eye. Lines for phenol represent fitting to zero-order kinetics.

experiments with Fe-Beta than with Fe-ZSM5. This is explained by the higher degree of adsorption and probably a positive shift in the ratio of 'reactive' vs. 'nonreactive' H_2O_2 decomposition in the case of Fe-Beta. The pH also decreased during the reaction in a similar way than in previous experiments with artificial solar light.

4. Conclusions

Results of the present study clearly point out that Fe-zeolites can be activated by light leading to an enhancement of the oxidation of organic compounds in a heterogeneous photo-Fenton reaction. Important improvements in terms of DOC reduction are obtained when solar light is applied. It is hypothesized, that similar to the homogeneous photo-Fenton process, light accelerates the production of reactive species ($OH^{\bullet}$ or ferryl) from H_2O_2 by enhancing the recycling of Fe^{III} to Fe^{II}. In addition, the pronounced positive effect of light on the degree of mineralization could be due to the fact that light facilitates the decomposition of rather stable complexes of iron and carboxylic acid intermediates (e.g. oxalic acid).

Comparing the two Fe-zeolites applied, Fe-ZSM5 and Fe-Beta, it can be concluded that Fe-ZSM5 produces reactive species at a higher rate but at the expense of a less favorable ratio of productive vs. non-productive H_2O_2 consumption. However, the rate of contaminant degradation and efficiency of H_2O_2 utilization can be largely improved by a high degree of adsorptive enrichment of the contaminant at the zeolite, as it was shown especially for imidacloprid. Thus, the selection of the most suitable Fe-zeolite catalyst for a certain water treatment task depends on the type of contaminants and the case-specific demands, e.g. high reaction rates or low H_2O_2 consumption.

In summary, this work demonstrates that Fe-zeolites could be suitable photo-Fenton catalysts for CPC photo-reactors using solar light. Compared to the homogeneous photo-Fenton process, the Fe-zeolites offer the following advantages: they (I) are active even at nearly neutral pH (which is relevant for waters with high buffer capacities), (II) allow to combine the principles of contaminant adsorption and oxidation and III) can be easily recycled due to a particle size in the μm range.

Acknowledgement

We thank Dr. R. Kurzhals (Süd-Chemie Zeolites, Bitterfeld, Germany) for providing the Fe-zeolites. This work was supported by PIEF-GA-2009-236583 (EU Marie Curie Fellowship, R.G.-O.) and JCI-2010-07104 (Ministerio de Ciencia e Innovación, Spain, Juan de la Cierva Fellowship, R.G.-O.)

References

[1] P.R. Gogate, A.B. Pandit, Advances in Environmental Research 8 (2004) 501–551.
[2] J.J. Pignatello, E. Oliveros, A. Mackay, Critical Reviews in Environmental Science and Technology 36 (2006) 1–84.
[3] J.M. Poyatos, M.M. Muñio, M.C. Almecija, J.C. Torres, E. Hontoria, F. Osorio, Water, Air, & Soil Pollution 205 (2010) 187–204.
[4] V. Camel, A. Bermond, Water Research 32 (1998) 3208–3222.
[5] M. Hartmann, S. Kullmann, H. Keller, Journal of Materials Chemistry 20 (2010) 9002–9017.
[6] S. Malato, P. Fernandez-Ibanez, M.I. Maldonado, J. Blanco, W. Gernjak, Catalysis Today 147 (2009) 1–59.
[7] H. Suty, C. Traversay, Water Science and Technology 49 (2004) 227–233.
[8] J.J. Pignatello, D. Liu, P. Huston, Environmental Science and Technology 33 (1999) 1832–1839.
[9] S. Navalon, M. Alvaro, H. Garcia, Applied Catalysis B: Environmental 99 (2010) 1–26.
[10] R. Gonzalez-Olmos, U. Roland, H. Toufar, F.-D. Kopinke, A. Georgi, Applied Catalysis B: Environmental 89 (2009) 356–364.
[11] A. Georgi, R. Gonzalez-Olmos, R. Köhler, F.-D. Kopinke, Separation Science and Technology 45 (2010) 1579–1586.
[12] A. Tomasevic, E. Kiss, S. Petrovic, D. Mijin, Desalination 262 (2010) 228–234.
[13] F. Duarte, L.M. Madeira, Separation Science and Technology 45 (2010) 1512–1520.
[14] M.B. Kasiri, A. Aleboyeh, H. Aleboyeh, Water Science and Technology 61 (2010) 1617–1627.
[15] M.B. Kasiri, A. Aleboyeh, H. Aleboyeh, Applied Catalysis B: Environmental 84 (2008) 9–15.
[16] A. Noorjahan, V.D. Kumari, A. Subrahmanyam, L. Panda, Applied Catalysis B: Environmental 57 (2005) 291–298.
[17] H. Kusic, N. Koprivanac, I. Selanec, Chemosphere 65 (2006) 65–73.
[18] E.V. Kuznetsova, E.N. Savinov, L.A. Vostrikova, G.V. Echevskii, Water Science and Technology 49 (2004) 109–116.
[19] M. Rios-Enriquez, N. Shahin, C. Duran-de-Bazua, J. Lang, E. Oliveros, S.H. Bossmann, A.M. Braun, Solar Energy 77 (2004) 491–501.
[20] C. Baerlocher, L.B. McCusker, D.H. Olson, Atlas of Zeolite Framework Types, Elsevier, Oxford OX2 8DP, UK, 2007.
[21] M. Kositzi, I. Poulios, S. Malato, J. Caceres, A. Campos, Water Research 38 (2004) 1147–1154.
[22] L. Prieto-Rodriguez, I. Oller, A. Zapata, A. Agüera, S. Malato, Catalysis Today 161 (2011) 247–254.
[23] A.L. Pham, C. Lee, F.M. Doyle, D.L. Sedlak, Environmental Science and Technology 43 (2009) 8930–8935.
[24] R. Gonzalez-Olmos, F. Holzer, F.-D. Kopinke, A. Georgi, Applied Catalysis A: General 398 (2011) 44–53.
[25] U. Bali, E.C. Çatalkaya, F. Sengül, Journal of Environmental Science and Health, Part A A38 (2003) 2259–2275.
[26] C. Chmelik, J. Kärger, Chemical Society Reviews 39 (2010) 4864–4884.
[27] PhysProp Database Demo, Syracuse Research Corporation, 1999.
[28] Solution Kinetics Database, NDRL/NIST.
[29] C. Zaror, C. Segura, H. Mansilla, M.A. Mondaca, P. Gonzalez, Environmental Technology 31 (2010) 1411–1416.
[30] C.S. Salazar, M.D. Labas, R.J. Brandi, A.E. Cassano, Chemosphere 66 (2007) 808–815.
[31] R. Aplin, A.J. Feitz, T.D. Waite, Water Science and Technology 44 (2001) 23–30.
[32] V. Kavitha, K. Palanivelu, Chemosphere 55 (2004) 1235–1243.